Soil Biology and Biochemistry 202 (2025) 109694

Contents lists available at ScienceDirect

Soil Biology and Biochemistry

journal homepage: www.elsevier.com/locate/soilbio

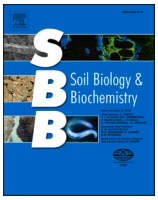

Evidence of the need for crop-specific N_2O emission factors

Akeem T. Shorunke, Bobbi L. Helgason *, Richard E. Farrell

Department of Soil Science, University of Saskatchewan, 51 Campus Drive, Saskatoon, SK, S7N 5A8, Canada

ARTICLE INFO

Keywords:
Nitrous oxide
Emission factor
Nitrogen cycling genes
Stable isotope
^{13}C-PLFA

ABSTRACT

Crop residues are an important source of N for subsequent crops and contribute to cropping system nitrous oxide (N_2O) emissions. Oilseed residues, particularly canola (*Brassica napus* L.), can instigate higher N_2O emissions compared to pulse and wheat crop residues but the reason for this disproportionate emission response is unknown. To determine the quantity and source of N_2O emissions, we conducted an incubation experiment (84 d) using ^{15}N and ^{13}C labelled residues of canola, wheat, flax, pea and investigated key N-cycling gene abundances, microbial abundance and community structure using PLFA and soil C and N dynamics. Residue addition of all types significantly increased microbial abundance and abundances of denitrification and nitrification genes. Canola residue resulted in significantly greater *nosZI* abundance. Lower incorporation of canola residue ^{13}C into PLFA and higher $^{13}CO_2$ emissions suggests that canola residue C was used less efficiently (i.e., less for growth and more for respiration), depleting O_2 and stimulating denitrification. The magnitude of N_2O emission from residue-amended soils was significantly higher ($p < 0.05$) than the unamended control soil and differed with residue type: canola > pea = wheat > flax > control. The canola residue emission factor was 1.56% of residue N – significantly higher than that of wheat (0.99%), pea (0.95%) and flax (0.18%). This higher canola emission factor resulted from greater residue-derived (1.47%) N_2O as well as residue-induced (0.65%) soil emissions. The combined use of stable isotope tracing of $^{15}N_2O$ and $^{13}CO_2$ and microbial characterization quantified differences in residue-derived N_2O emissions from common crops that were linked to differences in microbial abundance, community structure and activity.

1. Introduction

Soil nitrous oxide (N_2O) emissions are a result of microbially-mediated nitrification and denitrification acting on soil-, fertilizer- and/or crop residue-nitrogen (N) (Baggs and Philippot, 2010; Butterbach-Bahl et al., 2013). Published reports demonstrate that returning crop residues to the soil can produce either a stimulatory (Essich et al., 2020; Li et al., n.d.; Mutegi et al., 2010; Shang et al., 2011) or inhibitory effect (Ma et al., 2010; Sander et al., 2014) on N_2O emissions. A recent meta-analysis showed that compared to crop residue removal, residue incorporation increased N_2O emissions by an average of 43% and were best predicted by degradable fractions of specific residue types (e.g., water soluble carbon (C)) and total N (Abalos et al., 2022). Recently, the International Panel on Climate Change (IPCC) adopted Tier 1 emission factors of 0.016 for emissions of N_2O from synthetic fertilizers and 0.006 for organic amendments (including crop residues) in wet climates and an emission factor of 0.005 for both synthetic and organic inputs in dry climates (Hergoualc'h et al., 2021). Whereas this assumes that all crop residues contribute equally, several studies have reported differences in N_2O emissions among residue types (Li et al., 2021; Abalos et al., 2022; Janz et al., 2022; Lashermes et al., 2022).

A recent field study conducted in Saskatchewan, Canada, found that N_2O emissions can be higher for wheat grown on canola stubble than on either wheat or pea stubble (Lemke et al., 2018). A meta-analysis that compared winter oilseed rape found that annual emissions were 22% higher compared to winter cereals (Walter et al., 2015). In contrast, Begum et al. (2014) found lower emissions from canola compared to wheat and sorghum in an acidic soil. Likewise, a field study comparing canola and chickpea (Schwenke et al., 2010) found that cumulative emissions from the canola were 10-times greater than those from chickpea. Often, these disparities in N_2O emissions are attributed to differences in the quality of the crop residues but quality is not explicitly measured. A recent study by Lashermes et al. (2022) showed that total soil N_2O emissions during residue decomposition of nine field crops were strongly linked to their soluble neutral detergent content. However, in contrast to previously reported elevated emissions from canola,

* Corresponding author.
E-mail address: bobbi.helgason@usask.ca (B.L. Helgason).

https://doi.org/10.1016/j.soilbio.2024.109694
Received 8 August 2024; Received in revised form 10 December 2024; Accepted 13 December 2024
Available online 15 December 2024
0038-0717/© 2024 The Authors. Published by Elsevier Ltd. This is an open access article under the CC BY license (http://creativecommons.org/licenses/by/4.0/).

Table 1
Crop residue characteristics. Residue additions were based on shoot-to-root ratios determined from field studies in Saskatchewan (Gan et al., 2009).

Crop residue		Total N		Total C		C:N[a]	^{15}N		^{13}C	
Crop	(g kg^{-1})	%N	(mg N kg^{-1})	%C	(g C kg^{-1})		(atom%)	(μg kg^{-1})	(atom%)	(mg kg^{-1})
Above-ground residue (AGR)										
Canola	7.222	1.09	78.33	43.06	3.110	41:1	0.6283	492.2	1.2729	39.58
Flax	4.511	1.74	78.67	46.23	2.085	27:1	0.5640	443.7	1.2577	26.25
Pea	5.626	1.10	62.08	42.90	2.414	35:1	0.5718	355.0	1.2585	30.42
Wheat	5.624	0.87	49.08	42.06	2.366	49:1	0.5885	288.8	1.2333	29.17
Below-ground residue (BGR)										
Canola	1.832	0.86	15.83	42.66	0.781	– –	0.5515	87.3	1.1928	9.33
Flax	0.343	0.91	3.08	43.05	0.148	– –	0.5147	15.8	1.1972	1.75
Pea	1.090	1.91	20.75	41.65	0.454	– –	0.5161	107.1	1.1681	5.33
Wheat	0.657	0.81	5.33	43.91	0.288	– –	0.4993	26.7	1.1780	3.42

[a] Carbon to nitrogen ratio of a composite sample of the above-ground + below-ground residue.

they observed highest N_2O emissions from sugarbeet and mustard, with only very low N_2O emissions from rapeseed residues.

In addition to residue quality, the amount of N_2O emitted depends on several soil factors such as soil aeration and the availability of inorganic N and organic C substrates—all of which are affected by soil and crop management (Baggs, 2006; Basche et al., 2014; Rochette, 2008; Yamamoto et al., 2017). The decomposition of crop residues in the soil provides a source of readily available C and N that can stimulate microbial activity and, in turn, lead to increased N_2O production/emissions (Aulakh et al., 2000; Shang et al., 2011; Xia et al., 2014). As an organic N fertilizer, crop residues are subject to microbial N mineralization and eventual nitrification—during which N_2O can be produced (Baggs, 2011). Crop residues also affect denitrification by serving as a C and energy source for denitrifiers, thus enhancing N_2O production under anaerobic conditions (Chen et al., 2013). Residue decomposition may result in the development of anaerobic microsites in the soil by modifying soil aggregation and increasing microbial oxygen (O_2) consumption, driving the balance between nitrification, nitrifier-denitrification and heterotrophic denitrification (Bakken et al., 2012; Schaufler et al., 2010). Crop residue additions can also influence the ratio of N_2O to N_2 produced. For example, Li et al. (2013) reported that residue additions reduced soil N_2O production under O_2-limiting conditions and suggested that this was a result of enhanced complete denitrificaiton (i.e., reduction of N_2O to N_2). Thus, characterizing microbial community responses to the addition of different crop residues is necessary to improve residue managment and reduce residue-derived N_2O emissions.

Soil C and nutrient cycling processes are regulated by soil microorganisms through their influence on decomposition and incorporation of organic material (Cotrufo et al., 2013; Fanin et al., 2019; Schimel and Schaeffer, 2012). Understanding how substrate availability influences soil microbial community structure and function is important to determining the fate of C, N, and other nutrients during residue decomposition—and how this ultimately affects N_2O emissions. Changes in abundance, community structure and/or activity can all affect N_2O emissions. For example, Linton et al. (2020) found higher abundance and activity of bacterial functional groups that contribute to N cycling and N_2O emissions under long-term diverse crop rotations. However, in some cases quantifying gene abundance does not inform process rates or products (Barrat et al., 2022) which may be driven by soil environmental conditions influencing microbial activity, rather than genetic potential for N_2O production and reduction (Duan et al., 2018).

Stable isotope probing with ^{15}N can be used to differentiate sources N_2O–N emitted from soil (Baggs, 2008; Ferrari Machado et al., 2021; Hu et al., 2015; Machado et al., 2021). By quantifying the amount and proportion of $^{15}N_2O$ emitted and normalizing this to the proportion of residue N that had a ^{15}N label, the total quantity of residue-derived N_2O can be determined (Liu et al., 2024). This determination assumes that the ^{15}N was evenly distributed in the residue and that no isotopic discrimination occurred during N_2O production or consumption. Residue ^{13}C tracing into PLFA during decomposition can reveal differences in active decomposer communities (Arcand et al., 2017; Helgason et al., 2014). When combined with microbial functional gene and transcript quantification (e.g., Masta et al., 2023; Reimer et al., 2023) stable isotope tracking can provide additional information about the relative contribution of groups that produce and consume N_2O and evidence for the pathways responsible for emissions.

The objectives of the study were to (i) use ^{15}N- and ^{13}C-labelled residues of wheat, pea, flax and canola to quantify the sources of N_2O and carbon dioxide (CO_2) emissions; (ii) characterize abundance and community structure of residue ^{13}C-assimilating microorganisms; (iii) assess changes in the abundance of genes for key steps in the microbial nitrification and denitrification pathways; and (iv) explore relationships between microbial communities, soil chemical properties, and N_2O emissions. We hypothesized that (i) direct residue-derived N_2O emissions following the addition of canola residues would be greater than those following the addition of pea, wheat and flax residues, and (ii) differences in residue-derived N_2O emissions are related to changes in abundance of nitrifiers, denitrifiers and active crop residue decomposers.

2. Materials and methods

2.1. Laboratory incubation

Soil for the microcosm studies was collected from research plots at the Canada-Saskatchewan Irrigation Diversification Centre (CSIDC) in Outlook, SK (51°28′44 N 107°03′23W). The soil is classified as an Orthic Dark Brown Chernozem of the Bradwell association with a sandy loam texture, a pH of 7.5, EC of 0.86 dS cm^{-1}, and an organic matter content of 2.8%. The soil was collected from a depth of 0–10 cm in late spring from annual cropland previously cropped to spring wheat. The soil was air dried and screened to pass a 2-mm sieve and remove any visible plant residue, and then sent to *Farmers Edge Laboratories* (Winnipeg, MB) for analysis. Soil test results indicated that the soil was high in available N (119 kg NO_3–N ha^{-1}), P (78 kg P ha^{-1}), K (516 kg K ha^{-1}), and S (36 kg SO_4–S ha^{-1}). Total organic C (1.42%) and total N (0.19%) content of the soil (and residues) were determined in the Department of Soil Science, using a standard dry-combustion technique (McGill et al., 2007; Skjemstad and Baldock, 2007).

Residues of canola (*Brassica napus* L.; Dekalb 72-65 RR), flax (*Linum usitatissimum*; cv. CDC Bethune), pea (*Pisum sativum*; cv. CDC Treasure) and wheat (*Triticum aestivum*; AC Barrie) were dually labelled with ^{15}N and ^{13}C as described by (Shorunke, 2020; Supplemental Information). The treatments included a blank (no soil and no residue; used to obtain $\delta^{15}N$ values for the laboratory air); a control (soil with no residue; used to determine background emissions); and soil amended with one of four ^{15}N- and ^{13}C-labelled crop residues (canola, flax, pea, or wheat). Each treatment was replicated four times (n = 24), with the microcosms

arranged using a completely randomized design. An additional set of "destructively sampled" microcosms (5 treatments × 4 sampling times × 4 reps; n = 80) used for microbial analyses (see Section 2.4) also were included and gas sampled.

Prior to the start of the microcosm study, the soil was brought to (and maintained at) a gravimetric soil water content (GSWC) of 17% (approximately 55% water-holding capacity) to allow the soil microbial community to stabilize—during a 3-week pre-incubation period at room temperature—and eliminate the CO_2-flush that occurs on rewetting of a dried soil (Lee et al., 2007). At the end of the pre-incubation period, the $^{15}N/^{13}C$-labelled crop residues were incorporated into the soil at rates based on estimated average yields and straw-to-grain and straw-to-root estimates for the different crops on the Canadian prairies (Gan et al., 2009) (Table 1).

All treatment replicates were prepared individually by adding the residue (above- and below-ground residue) to an appropriate amount of moist soil (i.e., equivalent to 120 ± 0.5 g oven-dry weight) in the stainless-steel bowl of a Cuisinart® 5.5 qt. stand mixer; the sample was then homogenized by mixing (speed setting = 6) for 2 min. The residue-amended soil was then transferred into a 40-dram plastic vial, packed to a bulk density of 1.2 g cm^{-3}, wetted with enough water to bring it to a final volumetric water content equivalent to 60% WFPS, and placed in a 1-L Kilner® jar that was sealed with a polypropylene lid fitted with a self-sealing septum to allow for gas sampling. The jars were then incubated in the dark at room temperature (24 ± 2 °C) for *ca.* 84 d.

2.2. Gas sampling and analysis

Gas samples were collected throughout the 84-d incubation period but were sampled with greater frequency at the start of the experiment; i.e., at 0, 4, 18, 24, 36, 48, 97, 145, 193, 242, 290, 362, 483, 604, 727, 971, 1507 and 2025 h after incorporation of the residues. Headspace samples were collected from the microcosms through a sampling port consisting of a gray butyl rubber septum sealed into the lid and were collected using a 30-cc gas tight syringe. (Note: syringes used to sample the microcosms containing $^{15}N/^{13}C$-labelled residues were not used to sample the blank or control [non-labelled residue] microcosms.) Sampling involved collecting three gas samples from each microcosm: one 20-mL gas sample was collected and transferred to a pre-evacuated 12-mL Exetainer vial (Labco Inc.; Ceredigion, UK) to determine the total concentrations of N_2O and CO_2 using a SCION 456-GC gas chromatograph equipped with a ^{63}Ni electron capture detector (for N_2O) and thermal conductivity detector (for CO_2) (SCION Instruments, Edmonton, AB) (Farrell and Elliott, 2008; David et al., 2018). Two additional 30-mL gas samples were collected and immediately injected into pre-evacuated 22-mL Kimax™ glass vials (Fisher Scientific, Ottawa, ON) for isotopic gas analyses using Picarro isotopic $^{15}N_2O$ and $^{13}CO_2/^{13}CH_4$ analyzers (G-5131-*i* and G-2201-*i*, respectively; Picarro Inc., Santa Clara, CA) (Congreves et al., 2016, 2019). Nitrous oxide concentrations in the headspace often exceeded the upper limit of the Picarro G5131-*i* analyzer (i.e., 2 ppmv); consequently, samples containing >2 ppmv N_2O (determined using GC) were then diluted with *zero-air* and run on the Picarro G5131-*i* analyzer to obtain the isotopic signature ($\delta^{15}N$) of the N_2O. Dilution effects were accounted for when calculating the total N_2O concentrations. After each sampling event, the microcosms were placed in a fume hood and left open for 20 min to replenish the atmosphere with ambient air. The Kilner® jars were then resealed and returned to the incubator until the next sampling period, when the gas collection/analysis procedure was repeated.

Nitrous oxide production curves were derived by plotting cumulative N_2O–N emissions *vs*. time, and were interpreted using the response parameters Farrell et al. (2001) used to describe polymer mineralization: (i) MAX-N_2O, defined as the total cumulative N_2O–N evolved during the incubation; (ii) LAG, defined as the period of time between the initial closure of the microcosms (i.e., at t_0) and the start of the period of rapid N_2O production; (iii) r_{MAX}, defined as the slope of the linear least-squares regression line plotted between the end of the lag period and the start of the plateau region of the cumulative N_2O production curve (i.e., the point at which the R^2 for the least-squares regression line drops below 0.95); and (iv) t_{MAX}, defined as the time (h) required for N_2O production to plateau. The same response parameters were used to describe the cumulative CO_2 production curves.

Residue-derived emissions; i.e., N_2O–N or CO_2–C derived directly from the crop residues, were calculated using Equations (1) and (2).

$$EF_r = \frac{15_{Nr} - 15_{Nc}}{15_{Na}} \times 100 \quad (1)$$

$$RDE = \frac{EF_r}{100} \times N_a \quad (2)$$

where EF_r = emission factor for residue-derived N_2O; $^{15}N_r$ and $^{15}N_c$ are the cumulative amounts of N_2O–^{15}N (μg ^{15}N kg^{-1} soil) produced by the residue-amended and control (unamended) soils, respectively; $^{15}N_a$ is the total amount of ^{15}N added as plant residue; *RDE* = total residue-derived emissions (mg N kg^{-1} soil); and N_a is the total amount of N added as plant residue (mg N kg^{-1} soil). The emission factors and total residue-derived CO_2 emissions were calculated by substituting CO_2–^{13}C (mg ^{13}C kg^{-1} soil) and total CO_2–C (g ^{13}C kg^{-1} soil) for N_2O–^{15}N and total N_2O–N in the above equations. Residue-induced soil emissions (*RISE*) are defined as the increase in total emissions relative to the unamended control; i.e.,

$$RISE = (TE_r - TE_c) - RDE \quad (3)$$

where TE_r and TE_c are the total N_2O (or CO_2) emissions from the residue-amended and unamended control soils, respectively.

2.3. Soil microbial abundance and functional group analysis

Once gas sampling was completed for a given date, microbial community analyses were conducted using randomly selected microcosms that were destructively sampled after the 0, 48, 97 and 362 h gas samples were collected. Soils were stored at −80 °C until DNA extraction. DNA was extracted from 0.25 g of soil using DNeasy® PowerSoil® Pro kit (QIAGEN, Strasse, Germany) according to the manufacturer's instruction, and DNA extracts were stored at −80 °C. Prior to quantitative PCR, genomic DNA template concentrations were adjusted to 10 ng μL^{-1} after quantification with Qubit®2.0 Fluorometer with Qubit® dsDNA HS assay kit (Thermo Fisher Scientific, Waltham, MA USA). The qPCR products for archaeal and bacterial *amoA*, *nirS*, *nirK*, *nosZ* clade I and *nosZ* clade II were performed in triplicate with an ABI StepOnePlus Real-time PCR system (Life Technologies, Burlington, ON) using SYBR green detection chemistry. Reactions were performed using established primers and conditions (Table S7) as previously described by Reimer et al. (2023). Abundance of N cycling genes was calculated using single target standards amplified from bacterial pure culture genomic DNA, with the exception of nosZII which was a multiple standard target (Reimer et al., 2023). Targets were cloned using an Invitrogen TOPO TA Cloning® Kit (Life Technologies, Carlsbad, CA). A QIAprep Spin Miniprep kit (Qiagen, Mississauga, ON) was used to extract and linearize plasmid DNA which was then run on a 1% agarose gel. Bands containing the linearized plasmid and targets were excised and purified using a QIAquick Gel Extraction kit (Qiagen, Mississauga, ON) and quantified using a Qubit® 2.0 Fluorometer with the Qubit® dsDNA HS assay kit (Thermo Fisher Scientific, Waltham, MA USA). All standards were sequenced to confirm successful cloning of the target gene. A 10-fold dilution standard ranging between 10^2 and 10^9 was prepared and run in triplicate on each plate for each functional gene we measured (AOB*amoA*, AOA*amoA*, *nirK, nirS*, *nosZI*, *nosZII*).

Phospholipid fatty acid analysis (PLFA) was conducted according to the method described by Helgason et al. (2010, 2014), modified from Bligh and Dyer (1959) and White et al. (1979). ^{13}C–PLFA stable isotope

Table 2
Effect of canola, flax, pea and wheat residue addition on soil microbial abundance ($^{12}C+^{13}C$ PLFA) at four different sampling times.

Crop residues	Total PLFA	Bacteria	G+ve	G-ve	Actino.	Fungi	Stress 1	Stress 2
	nmol g^{-1} soil							
Control	54.48 d[a]	32.81 d	13.42d	13.59 d	5.81 b	0.68 e	0.40 a	0.37 a
Canola	88.04 a	52.69 a	19.89a	25.85 a	6.95 a	3.19 a	0.32 d	0.23 d
Flax	75.32 c	44.19 c	17.68c	19.91 c	6.54 a	2.40 c	0.37 b	0.28 b
Pea	84.02 ab	49.15 ab	19.12 ab	23.24 ab	6.79 a	2.90 b	0.34 c	0.24 c
Wheat	76.67 bc	44.98 bc	17.44bc	20.99 bc	6.55 a	1.90 d	0.35 c	0.26 bc
Time								
0	56.99 c	32.40 c	12.16 d	15.32 d	4.92 c	2.01 b	0.34 b	0.26 b
48	87.59 a	52.82 a	21.15 a	24.50 a	7.17 a	2.66 a	0.32 c	0.25 b
97	73.07 b	42.75 b	16.74 c	19.17 b	6.85 b	1.70 b	0.42 a	0.34 a
362	85.18 a	51.09 a	20.00 b	23.88 a	7.17 a	2.48 a	0.34 b	0.26 b
Crop residues	***[b]	***	***	***	**	***	***	***
Incubation Time	***	***	***	***	***	***	***	***
Crop residues x Incubation Time	***	***	***	***	NS[c]	NS	***	***

[a] Different letters within the same column indicate a significant difference between means.
[b] *,**,*** Significant at $p \leq 0.05$, 0.01, and 0.001, respectively.
[c] Not significant.

probing was used to determine differences in the microbial abundance and community structures of organisms that assimilated the residue-derived ^{13}C present in different residues-amended soils, while natural abundance of microbial biomass was determined using control. For PLFA analysis, soil samples were sieved, freeze-dried and fatty acids extracted from 4.0 g of lyophilized soil in a methanol/-chloroform/phosphate buffer mixture and then dried down under constant N_2 flow. Neutral, glyco- and phospho-lipids were separated using solid phase extraction columns (0.50 g Si; Varian Inc. Mississauga, ON), sequentially eluted with chloroform ($CHCl_3$), acetone [$(CH_3)_2CO$] and methanol (MeOH) respectively, and the phospholipid fraction dried under N_2 flow. With a solution of 1:1 methanol/toluene and methanolic potassium hydroxide (KOH) at 37 °C, phospholipids were methylated. The resulting fatty acid methyl esters (FAMEs) were analyzed using a Scion 436-GC gas chromatograph with an Agilent 25 m ultra 2 capillary column (J&W Scientific), and a Flame Ionization Detector (FID), using hydrogen UHP carrier gas. Peaks were identified using fatty acid standards and custom software and quantified based on the addition of a known concentration of the internal standard methyl nonadecanoate (19:0) (Drenovsky et al., 2004; Helgason et al., 2010). Total biomass was determined by addition of all named peaks calculated based on the peak area detected for each fatty acid, relative to that of a known quantity of the internal standard. Bacterial biomass was determined using thirteen biomarkers (i14:0, i15:0, a15:0, i16:0, 16:1v7c, 10Me16:0, i17:0, a17:0, cy17:0, 10Me17:0, 18:1v7c, 10Me18:0, and cy19:0), which are further separated to represent Gram-positive bacteria (G+ve) (i14:0, i15:0, a15:0, i16:0, i17:0, a17:0) and Gram-negative bacteria (G-ve) (16:1 ω7t, 16:1ω9c, 16:1ω7c, 18:1ω7c, 18:1ω9c, cy17:0, and cy19:0) (Macdonald et al., 2004). Fungal biomass was assessed using 18:2ω6,9c (Bååth and Anderson, 2003), and actinobacteria accessed using fatty acid 10Me16:0 and 10Me18:0. Physiological stress biomarkers were reported as the ratio of cy17:0 to 16:1ω7c (Stress 1) and cy19:0 to 18:1ω7c (Stress 2) (Arcand et al., 2016; Grogan and Cronan, 1997). All biomass values reported based on dry soil weight in units of nmol g^{-1} soil (Helgason et al., 2010; Hynes and Germida, 2012). The C isotope ratio of fatty acids was determined by GC-C-IRMS. DELTA^{PLUS} isotope ratio mass spectrometer (Thermo Fisher Scientific, Waltham, MA) coupled with a Hewlett Packard 6890 series II GC (Agilent, Palo Alto, CA) through a GC Combustion-III interface (Thermo Fisher Scientific, Waltham, MA). Reference CO_2 of known isotopic composition was injected at the beginning of each sample run and a standard mixture of eight fatty acids of known isotopic composition was run with every analysis period. ^{13}C enrichment of the fatty acid was corrected for the C atom derived from methanol (−43.96‰) during methylation. Total PLFA analysis by Scion 436-GC using custom software identified 60 FAMEs. Inadequate separation of some FAMEs during GC-C-IRMS analysis as a result of blending $\delta^{13}C$ signals resulted in identification of Isotopic ratios for 31, 40, 33 and 41 FAMEs at 0, 48, 97 and 362 h destructive sampling respectively, thus necessitate exclusion of the blended FAMEs in our analysis, following steps described by (Helgason et al., 2014). Also, the quantity and distribution of ^{13}C incorporated into individual PLFA ($^{13}C_{inc}$) were calculated as described by (Helgason et al., 2014).

$$^{13}C_{inc} = (F_R - F_C)*PLFA_s \quad (4)$$

where $PLFA_s$ is the amount (μg g^{-1}soil) of an individual PLFA ($^{13}C + ^{12}C$) from the residue amended soil as determined by GC-FID, F_C is the fraction of ^{13}C in an individual PLFA of un-amended soil and F_R if from ^{13}C residue amended soil and calculated as:

$$F = R/(R + 1) = {}^{13}C/({}^{13}C + {}^{12}C) \quad (5)$$

The C isotope ratio (R) was derived using GC-C-IRMS measurement, relative to VPDB standard as follows:

$$R = (\delta^{13}C/1000 + 1)*R_{VPDB} \quad (6)$$

The percentage distribution of incorporated ^{13}C in an individual fatty acid or biomarker functional groups (% $^{13}C_{M\text{-}DIST.}$) was calculated by dividing $^{13}C_{inc}$ (μg g^{-1} soil) in an individual (18:2ω6,9c) lipid or group of lipids (G-bacteria) by the total amount of $^{13}C_{inc}$ (μg g^{-1} soil) in all identified FAMEs at different destructive sampling period (Moore-Kucera and Dick, 2008).

$$\%^{13}C_{M\text{-}DIST} = ({}^{13}C\text{-}PLFA/\sum {}^{13}C\text{-}PLFA)*100 \quad (7)$$

2.4. Characterization of nutrient content and soil properties

Water-soluble organic C and N were measured at all destructive sampling times. Water extractable organic matter was extracted from 5 g of soil using 5 m*M* $CaCl_2$ solution (1:2 w/v) (Kalbitz et al., 2003; Zsolnay, 1996; Zsolnay, 2003), and extract filtered with 0.4 μm polycarbonate filter using glass vacuum filter unit. The concentration of total dissolved nitrogen (TDN) and total dissolved organic carbon (DOC) was measured using combustion/non-dispersive infrared gas analysis

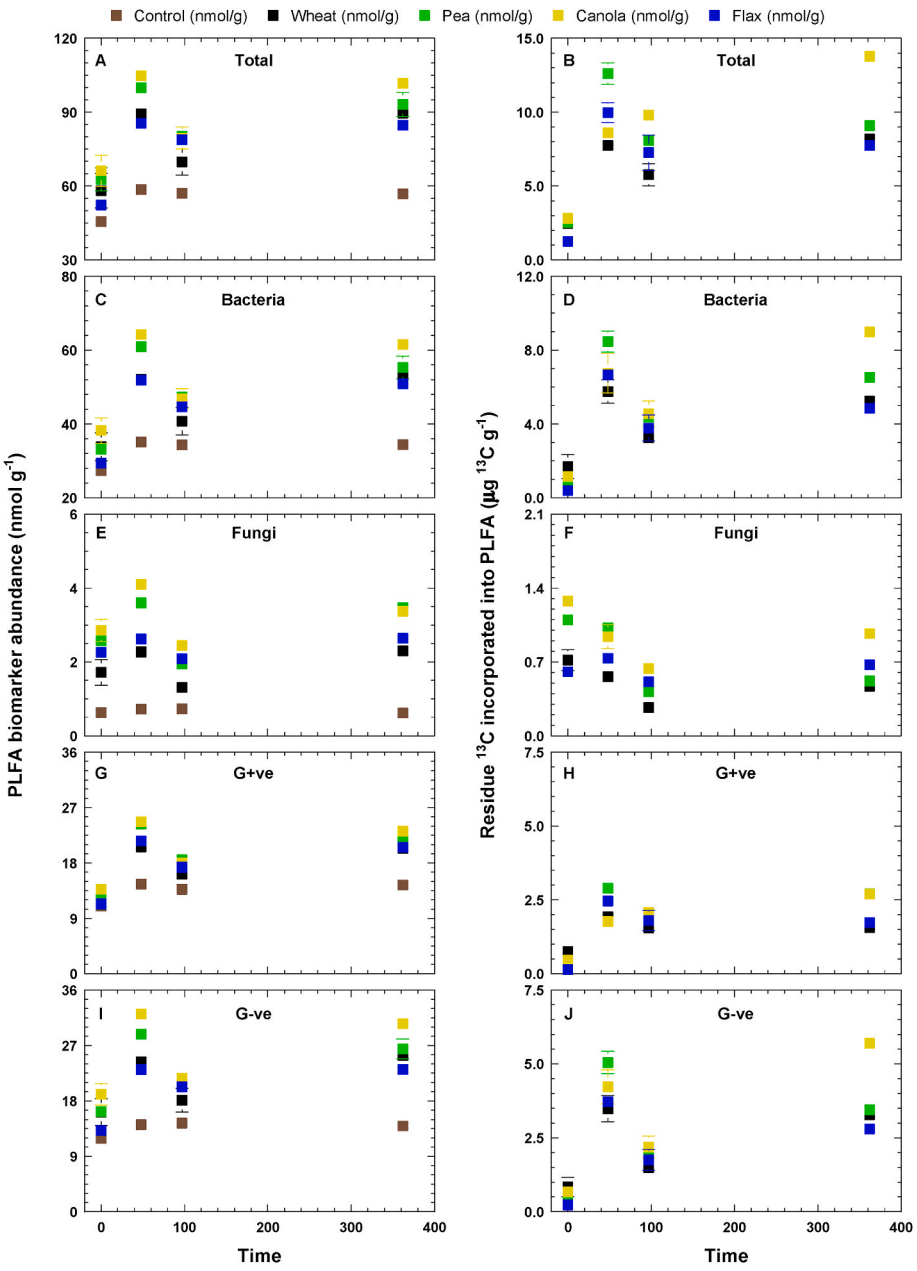

Fig. 1. Effect of ^{13}C-labelled residues of canola, flax, pea, and wheat phospholipids fatty acid (PLFA) biomarker abundance (panels A, C, E, G, & I) and incorporation of ^{13}C into the PLFA (panels B, D, F, H, & J). Error bars indicate standard error of the mean (n = 4).

method by using a total organic C analyzer (TOC-5000A, SHIMADZU). Exchangeable NO_3^- and NH_4^+ were extracted from 5 ± 0.1 g of soil by shaking in 50 mL of 2.0 *M* KCl (ratio 1:10). NO_3–N and NH_4–N in the extract were colorimetrically analyzed using segmented flow auto-analyzer (Technicon Autoanalyzer, Technicon Industrial Systems, Tarrytown, NY, USA).

2.5. Statistical analysis

The software package IBM SPSS statistics *v*. 26 was used to perform a linear mixed model analysis for repeated measures to determine significance of the differences between labelled residue applications for water-soluble organic C and N, N_2O emissions, ^{15}N–N_2O emissions, CO_2 emissions, ^{13}C–CO_2 emissions and N-functional gene abundances at $p <$ 0.05 as well as for correlation and multiple linear regression. All data were $\log_{10}$ transformed prior to regression analysis to satisfy normality and homogeneity of variance assumptions. Only predictor variables that were significant correlated ($p < 0.05$) with N_2O flux were included in the initial stepwise regression model. Least-significant difference (LSD) was used for post-hoc comparison of individual treatments. Principal coordinate analysis (PCoA) using PCOrd v.6 (MjM Software Gleneden Beach, OR) was used to analyze the community composition of the $\log_{10}$ transformed (mol% + 1) PLFA data and ^{13}C-PLFA % distribution. The Sørensen (Bray-Curtis) distance measure was used along with the PCoA analysis routine to randomize, calculate scores for variables by weighted average, and list statistics for all axes. Time of the day was selected as the source for random number seed. PERMANOVA was used to test for the effect of residue, time and their interaction on the total ^{12}C+^{13}C PLFA and active ^{13}C-PLFA community structure.

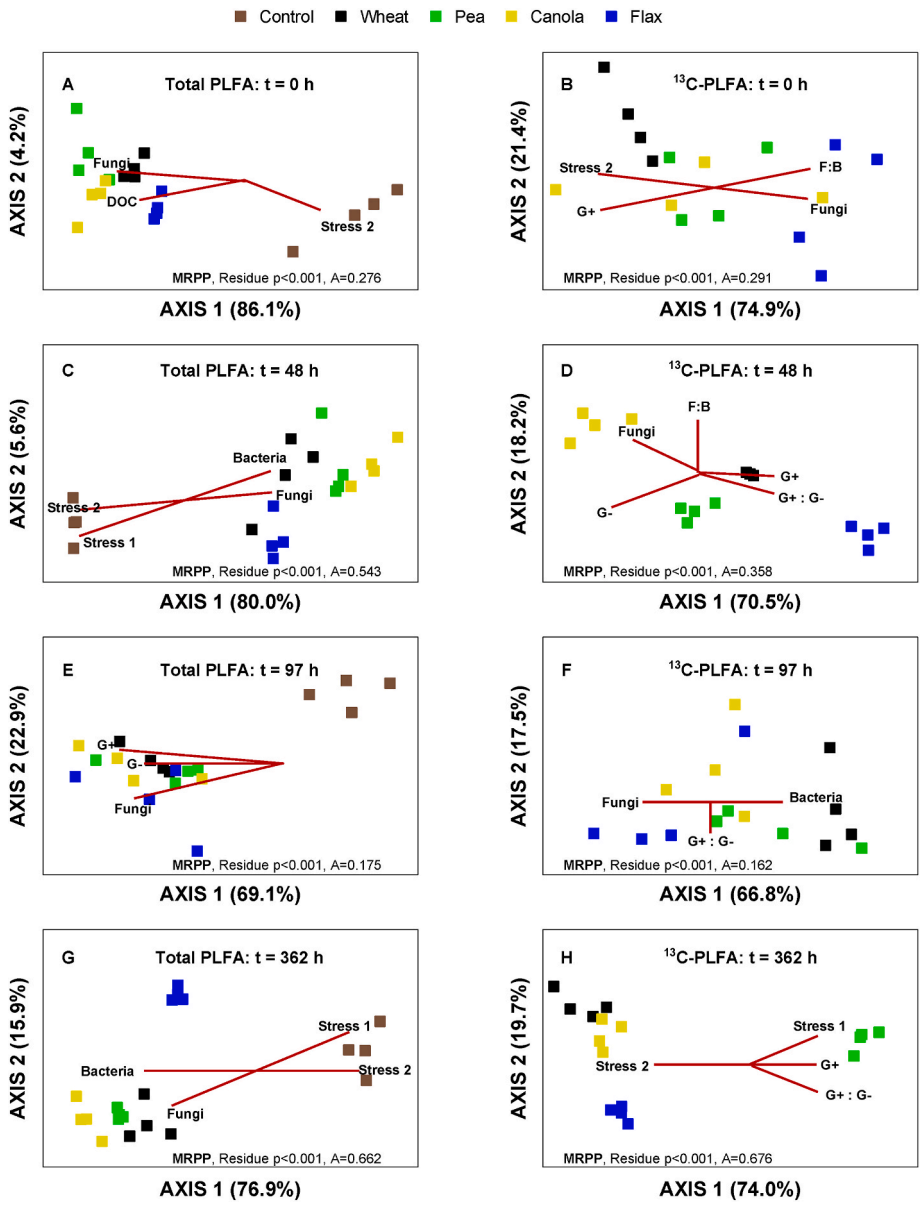

Fig. 2. Community structure of total ($^{12}C + {}^{13}C$) and ^{13}C phospholipid fatty acid (PLFA) distribution in microbial biomass at 0, 48, 97 and 362 h of soil amendment with labelled residues of canola, flax, pea and wheat.

3. Results

3.1. Soil microbial abundance and community structure

Addition of all crop residue types increased the abundance of total, bacterial and fungal PLFA biomarkers compared to control ($p < 0.001$; Table 2, Table S1). Abundance of all functional group biomarkers increased at 48 h followed by a decrease at 97 h and then increased again at 362 h. Canola residue addition resulted in the greatest biomarker increase and flax residues the least, for all functional groups except actinobacteria which was equal for all residue types.

The temporal dynamics of the effect of residue addition on total PLFA and the quantity of residue ^{13}C incorporated into the biomarker groups differed between residue types (Fig. 1, Table S1). Although addition of canola residues resulted in the highest total ($^{12}C+{}^{13}C$) PLFA, the total, bacterial, G+ve and G-ve biomarkers all contained more ^{13}C from pea than from other crop residues at 48 h when total biomass peaked for all residue types. Between 48 and 97 h, ^{13}C assimilation into microbial biomass increased for canola but decreased for pea, wheat and flax and was highest in canola at 362 h (Fig. 1A and B). These differences in residue ^{13}C assimilation between residue types demonstrate differences in C use efficiency (i.e. C used for growth *vs.* respiration) during peak N_2O production. There was an interaction between residue type and time for the quantity of residue ^{13}C assimilated within bacteria, fungi and G+ve groups (Fig. 1D–F, H) ($P < 0.002$). Comparison of total and ^{13}C-PLFA abundance shows that the proportion of growth derived from residue ^{13}C *vs.* soil C differed among residue types, particularly for pea and canola. For canola, less residue ^{13}C was detected in G+ve biomarkers and more in fungal biomarkers compared to pea at 48 and 97 h.

Residue-induced differences were likewise reflected as changes in the total and active community structure (Fig. 2; Table S2). At all time points, microbial communities in residue-amended soils differed from the control; differences between residue types were most apparent 48 and 362 h after residue addition (Fig. 2A–C, E, G). The community structure of active decomposers containing residue ^{13}C were likewise most distinct between residue types at 48 h (Fig. 2D). At 96 h after residue addition ^{13}C-PLFA profiles were more dispersed but became distinct again at 362 h with pea residue being most distinct from other

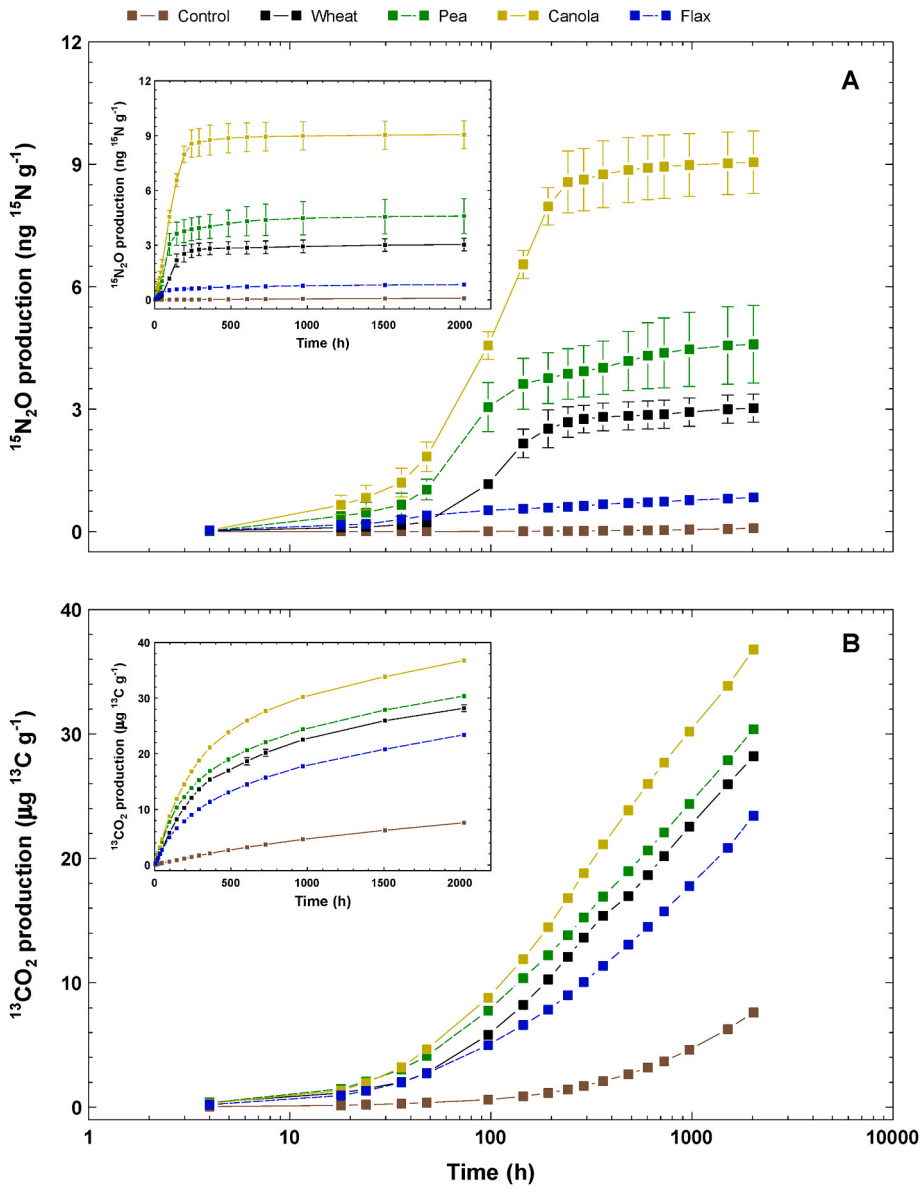

Fig. 3. (A) $^{15}N_2O$ production and (B) $^{13}CO_2$ production in soil microcosms amended with ^{15}N- and ^{13}C-labelled residues of canola, flax, pea, and wheat. Error bars indicate standard error of the mean (n = 4). Note: for the main figures, incubation time is plotted on a logarithmic (log_{10}) scale to show more detail during the initial stages of the incubation; however, typical GHG production curves—with time plotted on a linear scale—are presented as inserts.

residue types (Fig. 2F–H).

3.2. *Residue-derived vs. residue-induced N_2O and CO_2 emissions*

The concentration of $^{15}N_2O$ in the headspace of the incubation vessels provided a measure of the release of residue-derived N as N_2O. In general, $^{15}N_2O$ concentrations in the residue-amended microcosms increased following a short (4–18 h) lag period—with the subsequent rate of $^{15}N_2O$ production (r_{max}) decreasing in the order: canola ≈ pea > wheat ≈ flax (Fig. 3A; Table S3). Cumulative $^{15}N_2O$ emissions were greatest for the soil amended with canola residues and least for the soil amended with flax residues. Indeed, the canola residues released about 11-times more $^{15}N_2O$ than the flax residues, 3-times more than the wheat residues, and 2-times more than the pea residues (Table 3; Table S3). Expressed as a proportion of the total residue-^{15}N applied to the soils (i.e., as an emission factor [EF_r]), residue-derived emissions (RDE) ranged from 0.18% for flax to 1.56% for canola—with pea and wheat releasing 0.97 ± 0.02% of total residue-^{15}N as $^{15}N_2O$ (Table 3). Moreover, RDE accounted for 65–75% of total N_2O produced, with residue-induced soil emissions (RISE) accounting for 25–30% of total N_2O (Table 3).

Residue-derived $^{13}CO_2$ emissions are shown in Fig. 3B, with the response parameters summarized in Table S4. Soils amended with the different ^{13}C-labelled residues yielded $^{13}CO_2$ emission patterns that were similar—with the canola exhibiting a r_{max} value (0.061 ± 0.002 µg ^{13}C g^{-1} h^{-1}) that was 25–30% greater than that for soils amended with pea or wheat residue (0.046 ± 0.002 µg ^{13}C g^{-1} h^{-1}) and about twice that for the soil amended with flax residue (0.032 ± 0.002 µg ^{13}C g^{-1} h^{-1}). Cumulative $^{13}CO_2$ emissions from the residue-amended soils decreased in the order: canola > pea > wheat > flax; however, emission factors for the residue were relatively independent of residue type—averaging 56.0 ± 1.5% for canola and flax residue and 63.3 ± 0.3% for pea and wheat residue (Table 3). Direct RDE accounted for 75–95% of total respired $^{13}CO_2$ in the residue-amended microcosms—with CO_2 derived from the soil organic C pool accounting for the remainder of the total respired CO_2 (Table 3; Table S5). Moreover, residue additions

Table 3
Direct and indirect N_2O and CO_2 emissions resulting from soil amended with ^{15}N- and ^{13}C-labelled crop residues during an 84-day incubation at 60% water filled pore space (n = 4).

Crop residue	Residue N added		Cumulative N_2O[a]		EF_r[b] (%)	RDE[c] (μg N g^{-1})	RISE[d] (μg N g^{-1})
	(μg N g^{-1})	(ng ^{15}N g^{-1})	(μg N_2O–N g^{-1})	(ng N_2O–^{15}N g^{-1})			
Control	– –	– –	0.022 d	0.083 d	– –	– –	– –
Canola	94.16	579.5	2.139 a	9.048 a	1.56 a	1.47 a	0.65 a
Flax	81.75	459.5	0.215 cd	0.833 cd	0.18 c	0.14 c	0.05 c
Pea	82.83	462.1	1.101 b	4.590 b	0.99 b	0.82 b	0.26 b
Wheat	54.41	315.5	0.743 bc	3.023 bc	0.96 b	0.52 bc	0.20 b
Crop residue	Residue C added		Cumulative CO_2[a]		EF_r[b] (%)	RDE[c] (mg C g^{-1})	RISE[d,e] (mg C g^{-1})
	(mg C g^{-1})	(μg ^{13}C g^{-1})	(mg CO_2–C g^{-1})	(μg CO_2–^{13}C g^{-1})			
Control	– –	– –	0.543 d	7.625 e	– –	– –	– –
Canola	3.891	48.91	2.451 a	36.786 a	59.62 ab	2.32 a	−0.41 b
Flax	2.233	28.00	1.670 c	23.420 d	56.41 b	1.26 c	−0.13 a
Pea	2.868	35.75	2.067 b	30.378 b	63.64 a	1.83 b	−0.30 ab
Wheat	2.654	32.59	1.968 b	28.204 c	63.15 a	1.68 b	−0.25 ab

[a] Within columns, and for each gas, means followed by the same letter are not significantly different at $P \leq 0.05$ (Tukey's HSD).
[b] Emission factor; calculated as the percentage of applied ^{15}N released as N_2O–^{15}N or ^{13}C released as CO_2–^{13}C.
[c] Total residue-derived emissions = total residue-N added × (EF_r/100).
[d] Total residue-induced soil emissions = (N_2O–N from residue amended microcosm - N_2O–N from control microcosm) - RDE.
[e] Note: a negative value indicates that soil-derived CO_2 emissions in the residue-amended soils were less than those from the unamended soil (i.e., soil-derived emission = RISE + cumulative emission from the unamended control).

decreased the amount of C released from the soil organic C pool by as much as 76% for canola residues and as little as 24% for flax residues.

Production of CO_2 was high during the initial period of residue decomposition (Fig. 4B; Fig. S1), accompanied by a corresponding increase in O_2 consumption (Fig. 4A) and increase in N_2O production (Fig. 4C; Fig. S1). These dynamics changed rapidly over the first 96 h of incubation. Microbial respiration and N_2O production were greater in soils amended with canola residue and destructively sampled at 48 h and 97 h—with a correspondingly high O_2 consumption that would promote denitrifying conditions. Although microbial respiration (i.e., CO_2 production and O_2 depletion) in the soil amended with canola residue were higher at 362 h than those in the control microcosms (Fig. 4A and B), N_2O emissions were quite low (Fig. 4C)—presumably because the supply of readily-available residue-N had been largely depleted.

3.3. Changes in readily available C and N

The size of the inorganic soil N pools (i.e., NO_3^- and NH_4^+) varied with the type of residue added to the soil and over time (Fig. 5A & B; Table S5). Initial NO_3^- concentrations ranged from 140 to 165 mg NO_3^- kg^{-1} soil and were greatest in soil amended with pea residue and lowest in soil amended with flax residue and the unamended control (Fig. 5A). Regardless of residue type, NO_3^- concentrations decreased rapidly during the first 48–97 h before stabilizing. The soil amended with canola residue had the lowest NO_3^- concentrations ($P < 0.05$) compared to wheat, pea and flax and only the soil amended with wheat residue exhibited a significant ($P \leq 0.05$) decrease in NO_3^- concentration between 97 and 362 h (Fig. 5A). Addition of the crop residues resulted in an increase in initial soil NH_4^+ concentrations, with the greatest increase associated with the addition of flax (Fig. 3B). Regardless, soil NH_4^+ concentrations were relatively low throughout the incubation, ranging from 0.60 to 4.86 mg NH_4^+ kg^{-1} soil. Peak NH_4^+ concentrations occurred at 48 h for the canola residue (3.50 μg NH_4^+ g^{-1} soil) and at 97 h for the pea (4.39 mg NH_4^+ kg^{-1} soil) and wheat (4.07 mg NH_4^+ kg^{-1} soil) residues. Thereafter, NH_4^+ concentrations decreased and, by the end of the incubation, had returned to background levels.

Dissolved organic C concentrations increased significantly ($P < 0.001$) upon the addition of crop residues to the soil (Fig. 5C) with the greatest increases following the addition of canola and pea residues. Thereafter, however, DOC concentrations decreased rapidly during first 48–97 h of the incubation—when N_2O emissions were greatest—and changed little thereafter (Fig. 5C). Total dissolved nitrogen (TDN) concentrations increased in the control and residue-amended soils during the first 48 h (Fig. 5D) and then decreased sharply over the next 48 h with the largest decreases occurring in the soil amended with canola and wheat residues.

3.4. Abundance of N cycling genes

Addition of crop residues increased the abundance of all N cycling genes we measured by 48 h after residue addition for all crop types (Table 4). Only *nosZI* was influenced by crop residue type and was higher for canola than other residues (Table 4). There was no interaction of crop type with sampling time for amoA or nir genes, however temporal abundance dynamics varied for different genes (Table 4; Table S6). Abundance of archaeal *amoA* did not change after an initial increase at 48 h after residue addition but bacterial *amoA* increased at 48 h and then decreased. *nirS* peaked at 96 h while *nirK* abundance was highest at 48 h *nosZII* decreased at 48 and 96 h after residue addition but returned to original levels at 362 h while *nosZI* abundance increased upon residue addition and was highest at 362 h. Overall, the abundance of *nirK* was higher than *nirS,* except at 97 h and the abundance of *nosZII* was higher than *nosZI* at all timepoints. The ratio of *nirS* to *nirK* was highest at 96 h when N_2O emissions were also highest indicating a more dominant role for *nirS* denitrifiers in the production of N_2O during residue decomposition. The ratio of *nirS* to *nirK* genes to *nosZI* to *nosZII* genes was highest at 48 and 96 h when peak N_2O production occurred (Table 4).

3.5. Relationship between N_2O and ^{15}N–N_2O emissions and microbial biomarkers

Overall, *nirK* abundance was not correlated with N_2O emissions while *nirS* abundance was positively correlated with total N_2O (r = 0.62) and residue-derived ^{15}N–N_2O (r = 0.31) (Table 5). Abundance of *nosZI* was positively correlated with residue-derived ^{15}N–N_2O (r = 0.50) while *nosZII* was negatively correlated with total N_2O (r = −0.34). Analyzed separately by residue type, correlations revealed residue-specific differences in functional gene abundances. Specifically, all genes were negatively correlated with ^{15}N–N_2O emissions from wheat residues, except for *nosZII* (Table 5). In contrast, both *nirS* (r = 0.51) and *nosZI* (r = 0.83) were correlated with ^{15}N–N_2O from canola residues, along with a positive correlation between *nirS* and total N_2O (r = 0.87) and a negative correlation with *nosZII* (r = −0.83). Addition of pea residues resulted in a positive correlation of A*amoA* (r = 0.59) and *nirS* (r = 0.84)

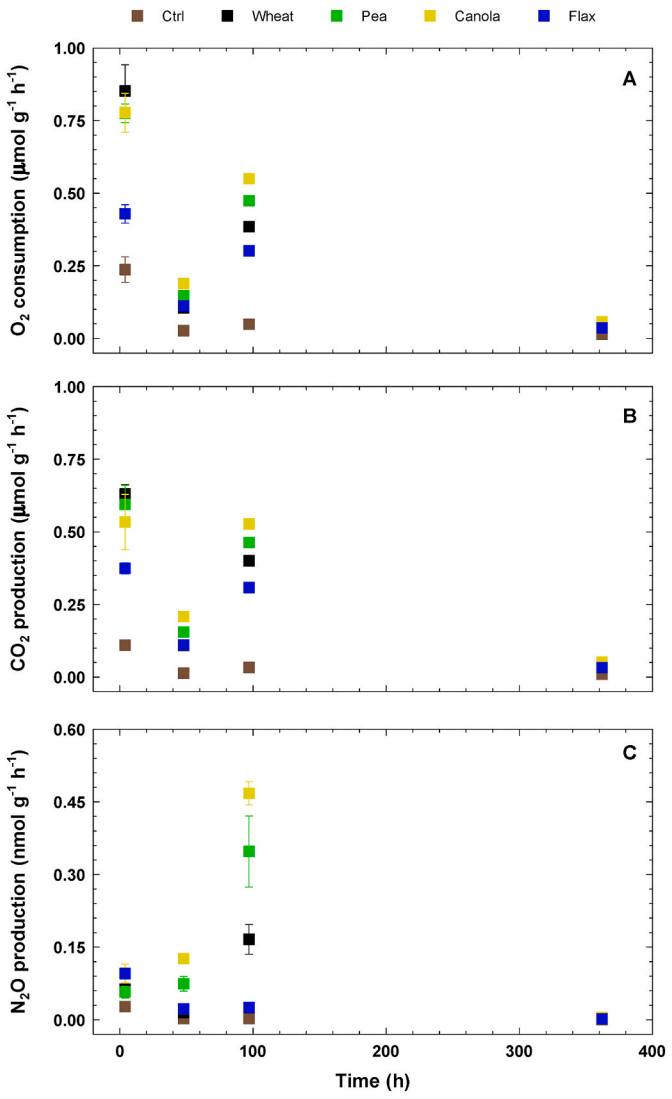

Fig. 4. Rates of O_2 consumption (A) and CO_2 (B) and N_2O production (C) in soil microcosms amended with residues of canola, flax, pea, and wheat. Error bars indicate standard error of the mean (n = 4).

with total N_2O and A*amoA* (r = 0.66), B*amoA* (r = 0.51), *nirS* (r = 0.59) and *nosZI* (r = 0.75) with ^{15}N–N_2O. Finally, addition of flax residues which had very low residue-derived and total emissions (Table 3) showed positive correlations of A*amoA* (r = 0.71) and *nirS* (r = 0.85) with total N_2O and *nosZI* with ^{15}N–N_2O (r = 0.80).

To test the predictive ability of soil pools on N_2O fluxes, we first used only soil pools in a multiple linear regression to determined that DOC, NH_4^+ and NO_3^- were strong predictors (R^2 = 0.68; p < 0.001) (not shown). Likewise, abundance of nosZI and the ratio of nirK + snirS to noszI + nosZII (nir:nos) also served as predictors of N_2O flux (R^2 = 0.47; p < 0.001) (not shown). When N cycling gene abundances were included with soil C and N pools, O_2 consumption and CO_2 respiration, CO_2 flux and nir:nos were the ultimately the strongest predictors of soil N_2O flux (R^2_{adj} = 0.87, p < 0.001) (Table 6). It is notable that there was high collinearity among soil pools and N gene abundances, demonstrating the coupling of microbial functional group population size with resource pools that contribute to N_2O production.

4. Discussion

Results from this study show that N_2O emissions during residue decomposition differ between residue types, with elevated N_2O related to microbial use efficiency of residue C. Canola residue induced substantially greater emissions than other residues: 1.56% of canola residue N was emitted as N_2O compared to ca. 0.95% for wheat and pea and 0.18% for flax. Most of the N_2O–N (ca. 68–75%) and CO_2–C (ca. 75–95%) was derived from the residues themselves, with the amounts of residue-^{13}C allocated to respiration *vs.* growth varying among residues. Specifically, more pea residue C was assimilated into biomass while more canola residue C was used for respiration, despite increases in total microbial biomass in both pea and canola residue-amended soils. The low C use efficiency of canola residues by the microbial community appeared to be coupled with the use of residue N for denitrification, resulting in disproportionately high N_2O production. Only the *nosZI* gene abundance and the *nosZI* to *nosZII* ratio differed between residue types, indicating that N cycling enzyme activity more than functional group population size was responsible for differences in N_2O emissions. Our results provide a mechanistic explanation for the higher-than-expected N_2O emissions from canola residues and provide further evidence supporting the need for crop-specific emission factors for residue-derived N_2O emissions.

4.1. Effects of residue on microbial abundance and activity

Crop residue incorporation into the soil can shift microbial abundance, community structure and activity with important consequences for biogeochemical processes, including gaseous N losses (Jackson et al., 2003). By providing both organic C and N, residues stimulate heterotrophic activity and can result in either N mineralization or immobilization. However, it is not only the availability of N that affects metabolism during decomposition. An increase in available C stimulates microbial metabolism, with a concomitant increase in O_2 consumption that can create anaerobic microsites driving denitrification (Beauchamp et al., 1989; Miller et al., 2008). At the same time, demand for alternative terminal electron acceptors increases and NO_3^-/NO_2^- is a more favorable electron acceptor than N_2O (Miller et al., 2008) thus increasing accumulation and subsequent N_2O emissions. Nitrous oxide emissions following residue addition can vary due to differences in the C:N ratio or decomposability of the crop residue (Duan et al., 2018).

Additions of fresh crop residue stimulate copiotrophic microorganisms that are characterized by high rates of growth and respiration (Bastian et al., 2009; Pascault et al., 2013). In contrast, oligotrophic microbial populations are characterized by lower rates of growth and respiration, and become increasingly dominant as the availability of labile C decreases during residue decomposition (Fanin et al., 2019; Fanin and Bertrand, 2016). Of the four residue types used in this study, canola, pea and wheat had C:N ratios that were much greater (ranging from 35:1 to 49:1) than that of flax (27:1) (Table 1). Kramer and Gleixner (2008) used stable isotope analysis to explain a shift in the proportion of G+ve and G-ve bacteria based on C availability. In line with this idea, many studies have shown an increase in the ratio of G+ve to G-ve bacteria with decreasing C availability following exhaustion of labile substrate (Breulmann et al., 2014; Fanin et al., 2019). This agrees with our findings where the abundance of Gram+ve *vs.* Gram-ve bacteria increased more for pea and wheat compared to canola residue.

A large proportion of residue C incorporation into the fungal biomass early during decomposition, was reported in previous studies (Arcand et al., 2016) and highlights the importance of fungi in the early stages of crop residue decomposition. It is possible that fungal denitrification contributed soil N_2O emissions, particularly in the early stages of canola decomposition (Chen et al., 2015; Phillips et al., 2016). Because fungi lack N_2O reductase capacity (Chen et al., 2013; Zhou et al., 2001; Zumft, 1997) they can produce but not reduce N_2O to N_2, however we did not assess fungal *nirK* abundance in our study.

All residue-amended soils produced larger amounts of N_2O compared to the unamended control soil, which agrees with previous studies that show increased N_2O emission after crop residue addition (Baggs et al., 2006; Gao et al., 2016). Large N_2O emissions in canola

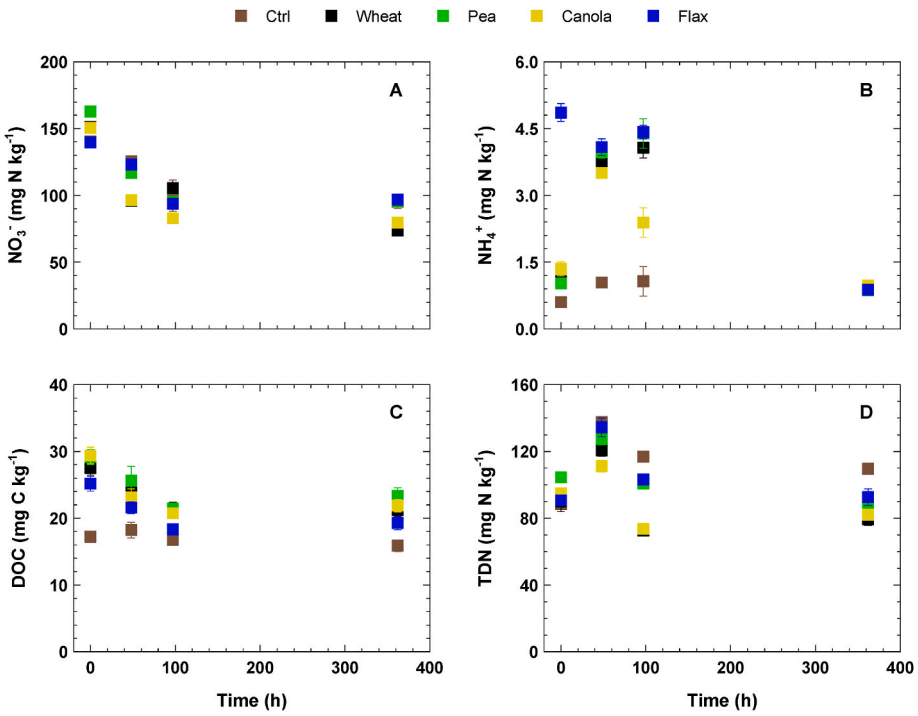

Fig. 5. Effect of wheat, pea, canola, and flax residue additions on soil NO_3^- (A), NH_4^+ (B), dissolved organic C (DOC) (C), and total dissolved N (TDN) (D). Error bars indicate standard error of the mean (n = 4).

Table 4
Effect of canola, flax, pea and wheat residue addition on N cycling genes at four different sampling times (n = 4).

Crop residues	A*amoA*	B*amoA*	*nirS*	*nirK*	*nosZ* I	*nosZ* II	*nirS*:*nirK*	*nosZ*I:*nosZ*II	*nir*:*nos*[d]
	log$_{10}$ gene copy # g^{-1} soil								
Control	9.37	8.09	7.31 b[a]	7.80 b	7.73 c	8.58	0.94	0.90 c	0.93
Canola	9.47	8.11	7.55 a	8.03 a	8.11 a	8.74	0.94	0.93 a	0.93
Flax	9.41	8.07	7.51 a	8.02 a	7.94 b	8.69	0.94	0.91 c	0.93
Pea	9.40	7.97	7.54 a	8.00 a	7.92 b	8.74	0.94	0.91 c	0.93
Wheat	9.39	8.02	7.46 a	8.03 a	7.95 b	8.74	0.93	0.91 c	0.93
Time									
0	9.14 b	7.85 c	6.72 c	7.63 c	7.50 c	8.93 a	0.88 c	0.84 b	0.87 c
48	9.52 a	8.23 a	7.40 b	8.55 a	7.93 b	8.46 b	0.87 bc	0.94 a	0.97 a
97	9.56 a	8.06 b	8.42 a	7.59 c	7.90 b	8.48 b	1.11 a	0.93 a	0.98 a
362	9.42 a	8.07 b	7.34 b	8.13 b	8.39 a	8.93 a	0.90 b	0.94 a	0.89 b
Crop residues (R)	NS[b]	NS	**[c]	**	**	*	NS	*	NS
Incubation Time (T)	***	***	***	***	***	***	***	***	***
R x T	NS	NS	NS	NS	NS	NS	NS	NS	NS

[a] Different letters within the same column indicate a significant difference between means.
[b] Not significant.
[c] *, **, *** Significant at $p \leq 0.05$, 0.01, and 0.001, respectively.
[d] nir:nos indicates (nirS + nirK)/(noszI + nosZII).

residue amended soils were associated with the highest level of CO_2 respiration and concomitant decreases in DOC and TDN from soil as well as residue C and N. This increased activity and utilization of DOC and TDN corresponded with higher microbial abundance than wheat or flax (but not pea), as well as higher residue-derived ^{13}C incorporation into fungi compared with other residue types. We were unable to determine whether the observed increase in denitrification-derived N_2O was driven by nitrifier-, heterotrophic bacterial- or fungal-denitrification.

4.2. N_2O emissions from crop residues

Similar to previous reports, the quantity of N_2O emissions emitted during decomposition of different crop residues varied substantially in our study. Field studies have assessed total soil N_2O emissions during residue decomposition, but these measurements include the influences of crop-specific N fertilizer additions (Abalos et al., 2022; Lemke et al., 2018), management factors such as tillage and residue incorporation (Ferrari Machado et al., 2021; Li et al., 2021) and are complicated by variable environmental conditions (Dueri et al., 2023). Combined, these factors have a strong influence on the magnitude and direction of N_2O emissions following residue addition when compared to control soils (Shan and Yan, 2013) but often cannot be decoupled from direct residue-derived emissions.

Decomposer activity following the incorporation of crop residues is

Table 5
Pearson correlation of total N_2O and residue-derived $^{15}N–N_2O$ emissions with N-cycling gene abundances.

	A*amoA*	B*amoA*	*nirS*	*nirK*	*nosZ* I	*nosZ* II
Overall						
N_2O	**0.26***[a]	0.12	**0.62****	−0.20	0.10	**−0.34****
$^{15}N–N_2O$	0.21	0.05	**0.31****	0.18	**0.50****	0.12
Canola						
N_2O	0.10	0.10	**0.87****	−0.47	−0.11	**−0.83****
$^{15}N–N_2O$	0.32	0.41	**0.51****	0.33	**0.83****	0.12
Wheat						
N_2O	0.54	0.11	**0.87****	−0.22	0.05	−0.31
$^{15}N–N_2O$	**−0.60***	**−0.60***	**−0.53***	**−0.60***	**−0.58***	**0.53***
Field Pea						
N_2O	**0.59***	0.34	**0.84****	−0.25	0.08	−0.43
$^{15}N–N_2O$	**0.66****	**0.51***	**0.59***	0.22	**0.75****	−0.08
Flax						
N_2O	**0.71***	0.04	**0.85****	0.21	−0.07	−0.50
$^{15}N–N_2O$	0.16	0.37	0.38	0.28	**0.80****	−0.33

[a] *,** Significant at $P \leq 0.05$ or 0.01, respectively.

Table 6
Multiple linear regression model to predict logN_2O flux (nmol g^{-1} soil h^{-1}) during residue decomposition.

Variable	B	95% CI	*β*	*t*	*p*
(Constant)	−0.189	[-0.349, −0.029]			
logCO_2 flux	1.363	[1.241, 1.485]	0.900	0.999	*p < 0.001*
log nir:noz	8.552	[5.517, 11.588]	0.227	0.999	*p < 0.001*

$R^2_{adj} = 0.87$ (N = 80, *p < 0.001*). CI = confidence interval for B.

influenced by the quality of native SOM and of the residue inputs themselves (Moreno-Cornejo et al., 2015) as well as by changes in microbial community structure that affects soil processes (Cavigelli and Robertson, 2001). Rapid early CO_2 respiration has been linked to increased N_2O emissions (Lashermes et al., 2022), which mirrors the response we observed to canola residue addition. Contrastingly, early N immobilization during high C:N residue decomposition has been proposed as a mechanism for reduced N_2O (Chen et al., 2013). As has been observed by others (Janz et al., 2022), residue N content or C:N ratio as a simple index of residue quality did not predict N_2O emissions in our study.

By using isotopically enriched residues we were able to quantify both direct residue-derived and indirect residue-induced emissions to show that while residue-induced emissions were proportionally similar in canola, pea, wheat, and flax, a much higher proportion of residue N was emitted as N_2O for canola and a much lower proportion for flax. By further measuring soil pools and microbial community responses to residue addition, a more complete understanding of the sources and drivers of residue-derived emissions can be achieved. A metanalysis by Abalos et al. (2022) found residue maturity to be a strong predictor, however in our case all residues were from mature crops. As such, we found that soil pools and N gene abundances served as predictors of N_2O fluxes during decomposition, rather than residue characteristics, with the strongest prediction by combining CO_2 flux with the ratio of N_2O production to consumption gene abundances (nir:nos).

4.3. Response of N cycling populations to residue addition

In agreement with previous studies (Gao et al., 2016; Tatti et al., 2014), we observed that the addition of crop residues significantly increased *nirS* and *nirK* gene abundances compared to the control. However, there were no differences in *nirS* and *nirK* genes copies between the different crop residue treatments themselves, despite differences in N_2O production indicating that major shifts in population size of N_2O producing populations were not responsible for either total or residue-derived N_2O. Similar patterns were observed for N_2O reduction genes, providing evidence that different residues did not simply increase the number of *nir* and *nos* containing organisms. Instead, residue quality likely influenced N_2O emissions through differences in activity both of organisms producing and consuming N_2O.

All steps in the denitrification pathway are not necessarily performed by same organism (Graf et al., 2014), but the genetic potential for N_2O production and consumption within a denitrifying community can inform the balance of N_2O production and consumption. As in Tosi et al. (2020) and Wu et al. (2017), we observed a positive relationship between *nirS* and N_2O emissions. However, we also observed a negative relationship between cumulative N_2O and *nirK*, similar to what has been reported by Jones et al. (2014) and Németh et al. (2014). The *nirK* bacteria seem to be more sensitive to changes in DOC and TDN than *nirS* denitrifiers, in agreement with Kandeler et al. (2006) and Bárta et al. (2010). The contrasting responses of *nosZ* clades I and II is in line with niche differentiation of the two clades in response to environmental conditions (Hallin et al., 2018). In our study the relative abundance of *nosZ* I *vs*. *nosZ* II increased with O_2 limitation and the increased consumption of DOC, TDN and NO_3^- which was most evident in soil amended with canola residue where the most N_2O was emitted.

4.4. Higher than expected N_2O emissions from canola residue

Our results are in accordance with previous reports of higher than expected N_2O emissions from canola residue decomposition in the field (Lemke et al., 2018). Here we were able to show that the majority of the N_2O was produced directly from residue N, likely by either nitrification or heterotrophic denitrification under low O_2 conditions triggered by high levels of respiration stimulated by canola residue C. Previous reports have suggested that glucosinolates and their derivatives have the potential to reduce N_2O emissions by reducing nitrification (Balvert et al., 2017; Bending and Lincoln, 2000). In contrast, Gao et al. (2022) observed increased soil N_2O emissions when glucosinolate derivative thiocyanate was applied together with artificial urine. Balvert et al. (2018) observed that N_2O from urea was reduced by the addition of glucosinolate-containing brassica residues. However, they were unable to determine the mechanism by which the reduction occurred and noted residue incorporation resulted in greater overall N_2O emissions similar to what we observed in our study.

Canola did not have a narrow C:N compared to the other residues. However, the form of available C for denitrification is known to influence N_2O emissions (Curtright and Tiemann, 2023). Using single substrate C sources, Giles et al. (2017) also observed the differences in CUE influenced N_2O emissions as a result of substrate-dependent partitioning of C between growth and respiration. We did not characterize the composition of the water extractable C from residues used in this study, but Surey et al. (2020) showed that the composition of water extractable organic matter from different plant residues was linked to "hot moments" of N_2O emissions by denitrification. Our study suggests that the higher-than expected N_2O emissions from canola result from denitrification, driven by microbial C use of residue C, though we were unable to determine whether nitrifiers, heterotrophic denitrifiers or fungi were the predominant source.

5. Conclusions

We quantified the impact of crop residue on N_2O emissions during decomposition of canola, wheat, pea and flax residues. Increased abundance and activity, more than changes in community structure were responsible for the differences, particularly the greater than expected N_2O emissions from canola residues. Specifically, canola residue C fueled high respiration immediately following addition, depleting O_2 and increasing the demand for NO_3^-/NO_2^- as terminal electron acceptors. The resulting increase in denitrification, coupled with lower *nosZII* gene abundance suggests both greater production and less consumption of N_2O from canola residues. Carbon:nitrogen ratio as a simple index of

residue quality did not explain these differences which were more strongly related to C than N in the residues. High quality pea residue appeared to result in greater C use efficiency during initial residue decomposition with more residue C incorporated into biomass growth and lower N_2O emissions, compared to canola. Our results support previous findings that a universal emission factor for N_2O from different types of crop residue N is not suitable for estimating this important source of agroecosystem N_2O emissions.

CRediT authorship contribution statement

Akeem T. Shorunke: Writing – review & editing, Writing – original draft, Visualization, Investigation, Formal analysis. **Bobbi L. Helgason:** Writing – review & editing, Visualization, Supervision, Resources, Project administration, Methodology, Funding acquisition, Formal analysis, Conceptualization. **Richard E. Farrell:** Writing – original draft, Visualization, Supervision, Resources, Project administration, Methodology, Funding acquisition, Formal analysis, Conceptualization.

Funding

This work was supported the Saskatchewan Ministry of Agriculture (Project 20150083 - Identifying the mechanisms responsible for the greater than expected residue-induced N_2O emissions from canola and flax).

Declaration of competing interest

The authors declare that they have no known competing financial interests or personal relationships that could have appeared to influence the work reported in this paper.

Acknowledgements

We acknowledge that this research was carried out on Treaty Six Territory and the Homeland of the Métis. We pay our respect to the First Nation and Métis ancestors of this place and reaffirm our relationship with one another. We are grateful to *Prairie Environmental Agronomy Research Laboratory (PEARL)* group in the Department of Soil Science at the University of Saskatchewan for labelling of the residues used in this study. We are grateful to Min Yu for technical assistance with qPCR assays of the nosZII gene. We also acknowledge the financial support that made this research work possible, from Agriculture and Agri-Food Canada and the Government of Saskatchewan, Agriculture and Development Fund.

Appendix A. Supplementary data

Supplementary data to this article can be found online at https://doi.org/10.1016/j.soilbio.2024.109694.

References

Abalos, D., Recous, S., Butterbach-Bahl, K., De Notaris, C., Rittl, T.F., Topp, C.F.E., Petersen, S.O., Hansen, S., Bleken, M.A., Rees, R.M., Olesen, J.E., 2022. A review and meta-analysis of mitigation measures for nitrous oxide emissions from crop residues. Science of the Total Environment 828, Scopus. https://doi.org/10.1016/j.scitotenv.2022.154388.

Arcand, M.M., Helgason, B.L., Lemke, R.L., 2016. Microbial crop residue decomposition dynamics in organic and conventionally managed soils. Applied Soil Ecology. https://doi.org/10.1016/j.apsoil.2016.07.001.

Arcand, M.M., Levy-Booth, D.J., Helgason, B.L., 2017. Resource legacies of organic and conventional management differentiate soil microbial carbon use. Frontiers in Microbiology 8 (NOV). https://doi.org/10.3389/fmicb.2017.02293.

Aulakh, M.S., Khera, T.S., Doran, J.W., 2000. Mineralization and denitrification in upland, nearly saturated and flooded subtropical soil II. Effect of organic manures varying in N content and C:N ratio. Biology and Fertility of Soils. https://doi.org/10.1007/s003740050641.

Bååth, E., Anderson, T.H., 2003. Comparison of soil fungal/bacterial ratios in a pH gradient using physiological and PLFA-based techniques. Soil Biology and Biochemistry 35 (7), 955–963. https://doi.org/10.1016/S0038-0717(03)00154-8.

Baggs, E.M., 2006. Partitioning the components of soil respiration: a research challenge. Plant and Soil 284 (1–2), 1–5. https://doi.org/10.1007/s11104-006-0047-7.

Baggs, E.M., 2008. A review of stable isotope techniques for N2O source partitioning in soils: recent progress, remaining challenges and future considerations. Rapid Communications in Mass Spectrometry 22 (11), 1664–1672. https://doi.org/10.1002/rcm.3456.

Baggs, E.M., 2011. Soil microbial sources of nitrous oxide: recent advances in knowledge, emerging challenges and future direction. In: Current Opinion in Environmental Sustainability. https://doi.org/10.1016/j.cosust.2011.08.011.

Baggs, E.M., Rees, R.M., Smith, K.A., Vinten, A.J.A., 2006. Nitrous oxide emission from soils after incorporating crop residues. Soil Use & Management. https://doi.org/10.1111/j.1475-2743.2000.tb00179.x.

Baggs, E., Philippot, L., 2010. Microbial terrestrial pathways to nitrous oxide. In: Nitrous Oxide and Climate Change. https://doi.org/10.4324/9781849775113.

Bakken, L.R., Bergaust, L., Liu, B., Frostegård, Å., 2012. Regulation of denitrification at the cellular level: a clue to the understanding of N2O emissions from soils. Philosophical Transactions of the Royal Society B: Biological Sciences. https://doi.org/10.1098/rstb.2011.0321.

Balvert, S.F., Luo, J., Schipper, L.A., 2017. Do glucosinolate hydrolysis products reduce nitrous oxide emissions from urine affected soil? Science of The Total Environment 603–604, 370–380. https://doi.org/10.1016/J.SCITOTENV.2017.06.089.

Balvert, S.F., Luo, J., Schipper, L.A., 2018. Can incorporating Brassica tissues into soil reduce nitrification rates and nitrous oxide emissions? Journal of Environmental Quality 47 (6), 1436–1444. https://doi.org/10.2134/jeq2018.04.0143.

Barrat, H.A., Charteris, A.F., Le Cocq, K., Abadie, M., Clark, I.M., Chadwick, D.R., Cardenas, L., 2022. N2O hot moments were not driven by changes in nitrogen and carbon substrates or changes in N cycling functional genes. European Journal of Soil Science 73 (1), e13190. https://doi.org/10.1111/ejss.13190.

Bárta, J., Melichová, T., Vaněk, D., Picek, T., Šantrůčková, H., 2010. Effect of pH and dissolved organic matter on the abundance of nirK and nirS denitrifiers in spruce forest soil. Biogeochemistry. https://doi.org/10.1007/s10533-010-9430-9.

Basche, A.D., Miguez, F.E., Kaspar, T.C., Castellano, M.J., 2014. Do cover crops increase or decrease nitrous oxide emissions? A meta-analysis. Journal of Soil and Water Conservation. https://doi.org/10.2489/jswc.69.6.471.

Bastian, F., Bouziri, L., Nicolardot, B., Ranjard, L., 2009. Impact of wheat straw decomposition on successional patterns of soil microbial community structure. Soil Biology and Biochemistry. https://doi.org/10.1016/j.soilbio.2008.10.024.

Beauchamp, E.G., Trevors, J.T., Paul, J.W., 1989. Carbon sources for bacterial denitrification. https://doi.org/10.1007/978-1-4613-8847-0_3.

Begum, N., Guppy, C., Herridge, D., Schwenke, G., 2014. Influence of source and quality of plant residues on emissions of N2O and CO2 from a fertile, acidic Black Vertisol. Biology and Fertility of Soils 50 (3), 499–506. https://doi.org/10.1007/s00374-013-0865-8.

Bending, G.D., Lincoln, S.D., 2000. Inhibition of soil nitrifying bacteria communities and their activities by glucosinolate hydrolysis products. Soil Biology and Biochemistry 32 (8), 1261–1269. https://doi.org/10.1016/S0038-0717(00)00043-2.

Bligh, E.G., Dyer, W.J., 1959. A rapid method of total lipid extraction and purification. Canadian Journal of Biochemistry and Physiology 37 (8), 911–917. https://doi.org/10.1139/o59-099.

Breulmann, M., Masyutenko, N.P., Kogut, B.M., Schroll, R., Dörfler, U., Buscot, F., Schulz, E., 2014. Short-term bioavailability of carbon in soil organic matter fractions of different particle sizes and densities in grassland ecosystems. Science of the Total Environment. https://doi.org/10.1016/j.scitotenv.2014.07.080.

Butterbach-Bahl, K., Baggs, E.M., Dannenmann, M., Kiese, R., Zechmeister-Boltenstern, S., 2013. Nitrous oxide emissions from soils: how well do we understand the processes and their controls? Philosophical Transactions of the Royal Society B: Biological Sciences. https://doi.org/10.1098/rstb.2013.0122.

Cavigelli, M.A., Robertson, G.P., 2001. Role of denitrifier diversity in rates of nitrous oxide consumption in a terrestrial ecosystem. Soil Biology and Biochemistry. https://doi.org/10.1016/S0038-0717(00)00141-3.

Chen, H., Li, X., Hu, F., Shi, W., 2013. Soil nitrous oxide emissions following crop residue addition: a meta-analysis. Global Change Biology. https://doi.org/10.1111/gcb.12274.

Chen, H., Mothapo, N.V., Shi, W., 2015. Fungal and bacterial N2O production regulated by soil amendments of simple and complex substrates. Soil Biology and Biochemistry. https://doi.org/10.1016/j.soilbio.2015.02.018.

Congreves, K.A., Dutta, B., Grant, B.B., Smith, W.N., Desjardins, R.L., Wagner-Riddle, C., 2016. How does climate variability influence nitrogen loss in temperate agroecosystems under contrasting management systems? Agriculture, Ecosystems & Environment. https://doi.org/10.1016/j.agee.2016.04.025.

Congreves, K.A., Phan, T., Farrell, R.E., 2019. A new look at an old concept: using 15N2O isotopomers to understand the relationship between soil moisture and N2O production pathways. Soil. https://doi.org/10.5194/soil-5-265-2019.

Cotrufo, M.F., Wallenstein, M.D., Boot, C.M., Denef, K., Paul, E., 2013. The Microbial Efficiency-Matrix Stabilization (MEMS) framework integrates plant litter decomposition with soil organic matter stabilization: do labile plant inputs form stable soil organic matter? Global Change Biology. https://doi.org/10.1111/gcb.12113.

Curtright, A.J., Tiemann, L.K., 2023. Chemical identity of carbon substrates drives differences in denitrification and N_2O reduction within agricultural soils. Soil Biology and Biochemistry 184, 109078. https://doi.org/10.1016/j.soilbio.2023.109078.

David, C., Lemke, R., Helgason, W., Farrell, R.E., 2018. Current inventory approach overestimates the effect of irrigated crop management on soil-derived greenhouse gas emissions in the semi-arid Canadian Prairies. Agricultural Water Management. https://doi.org/10.1016/j.agwat.2018.06.006.

Drenovsky, R.E., Elliott, G.N., Graham, K.J., Scow, K.M., 2004. Comparison of phospholipid fatty acid (PLFA) and total soil fatty acid methyl esters (TSFAME) for characterizing soil microbial communities. Soil Biology and Biochemistry 36 (11), 1793–1800. https://doi.org/10.1016/j.soilbio.2004.05.002.

Duan, Y.F., Hallin, S., Jones, C.M., Priemé, A., Labouriau, R., Petersen, S.O., 2018. Catch crop residues stimulate N2O emissions during spring, without affecting the genetic potential for nitrite and N2O reduction. Frontiers in Microbiology. https://doi.org/10.3389/fmicb.2018.02629.

Dueri, S., Léonard, J., Chlebowski, F., Rosso, P., Berg-Mohnicke, M., Nendel, C., Ehrhardt, F., Martre, P., 2023. Sources of uncertainty in simulating crop N2O emissions under contrasting environmental conditions. Agricultural and Forest Meteorology 340, 109619. https://doi.org/10.1016/j.agrformet.2023.109619.

Essich, L., Nkebiwe, P.M., Schneider, M., Ruser, R., 2020. Is crop residue removal to reduce N2O emissions driven by quality or quantity? A field study and meta-analysis. Agriculture 10 (11). https://doi.org/10.3390/agriculture10110546. Article 11.

Fanin, N., Bertrand, I., 2016. Aboveground litter quality is a better predictor than belowground microbial communities when estimating carbon mineralization along a land-use gradient. Soil Biology and Biochemistry. https://doi.org/10.1016/j.soilbio.2015.11.007.

Fanin, N., Kardol, P., Farrell, M., Nilsson, M.C., Gundale, M.J., Wardle, D.A., 2019. The ratio of Gram-positive to Gram-negative bacterial PLFA markers as an indicator of carbon availability in organic soils. Soil Biology and Biochemistry. https://doi.org/10.1016/j.soilbio.2018.10.010.

Farrell, R.E., Adamczyk, T.J., Broe, D.C., Lee, J.S., Briggs, B.L., Gross, R.A., McCarthy, S. P., Goodwin, S., 2001. Biodegradable Bags Comparative Performance Study: A Multi-tiered Approach to Evaluating the Compostability of Plastic Materials. In: ACS Symposium Series 786. American Chemical Society, Washington, DC, pp. 337–375.

Farrell, R.E., Elliott, J.A., 2008. Soil Air. In: Carter, M.R., et al. (Eds.), *Soil Sampling and Methods of Analysis*, 2nd Edition. Canadian Society of Soil Science, Boca Raton, FL, pp. 833–850.

Ferrari Machado, P.V., Farrell, R.E., Bell, G., Taveira, C.J., Congreves, K.A., Voroney, R. P., Deen, W., Wagner-Riddle, C., 2021. Crop residues contribute minimally to spring-thaw nitrous oxide emissions under contrasting tillage and crop rotations. Soil Biology and Biochemistry 152, 108057. https://doi.org/10.1016/j.soilbio.2020.108057.

Gan, Y.T., Campbell, C.A., Janzen, H.H., Lemke, R.L., Basnyat, P., McDonald, C.L., 2009. Carbon input to soil from oilseed and pulse crops on the Canadian prairies. Agriculture, Ecosystems & Environment. https://doi.org/10.1016/j.agee.2009.04.014.

Gao, J., Li, M.M., Zhao, G., 2022. Thiocyanate increases the nitrous oxide formation process through modifying the soil bacterial community. Journal of the Science of Food and Agriculture 102 (6), 2321–2329. https://doi.org/10.1002/jsfa.11570.

Gao, J., Xie, Y., Jin, H., Liu, Y., Bai, X., Ma, D., Zhu, Y., Wang, C., Guo, T., 2016. Nitrous oxide emission and denitrifier abundance in two agricultural soils amended with crop residues and urea in the North China Plain. PLoS One. https://doi.org/10.1371/journal.pone.0154773.

Giles, M.E., Daniell, T.J., Baggs, E.M., 2017. Compound driven differences in N2 and N2O emission from soil; the role of substrate use efficiency and the microbial community. Soil Biology and Biochemistry 106, 90–98. https://doi.org/10.1016/j.soilbio.2016.11.028.

Graf, D.R.H., Jones, C.M., Hallin, S., 2014. Intergenomic comparisons highlight modularity of the denitrification pathway and underpin the importance of community structure for N2O emissions. PLoS One. https://doi.org/10.1371/journal.pone.0114118.

Grogan, D.W., Cronan, J.E., 1997. Cyclopropane ring formation in membrane lipids of bacteria. Microbiology and Molecular Biology Reviews 61 (4), 429–441.

Hallin, S., Philippot, L., Löffler, F.E., Sanford, R.A., Jones, C.M., 2018. Genomics and ecology of novel N 2 O-reducing microorganisms. Trends in Microbiology. https://doi.org/10.1016/j.tim.2017.07.003.

Helgason, B.L., Gregorich, E.G., Janzen, H.H., Ellert, B.H., Lorenz, N., Dick, R.P., 2014. Long-term microbial retention of residue C is site-specific anddepends on residue placement. Soil Biology and Biochemistry. https://doi.org/10.1016/j.soilbio.2013.10.002.

Helgason, B.L., Walley, F.L., Germida, J.J., 2010. Long-term no-till management affects microbial biomass but not community composition in Canadian prairie agroecosytems. Soil Biology and Biochemistry. https://doi.org/10.1016/j.soilbio.2010.08.015.

Hergoualc'h, K., Mueller, N., Bernoux, M., Kasimir, Ä., van der Weerden, T.J., Ogle, S.M., 2021. Improved accuracy and reduced uncertainty in greenhouse gas inventories by refining the IPCC emission factor for direct N2O emissions from nitrogen inputs to managed soils. Global Change Biology 27 (24), 6536–6550. https://doi.org/10.1111/gcb.15884.

Hu, H.-W., Chen, D., He, J.-Z., 2015. Microbial regulation of terrestrial nitrous oxide formation: understanding the biological pathways for prediction of emission rates. FEMS Microbiology Reviews 39 (5), 729–749. https://doi.org/10.1093/femsre/fuv021.

Hynes, H.M., Germida, J.J., 2012. Relationship between ammonia oxidizing bacteria and bioavailable nitrogen in harvested forest soils of central Alberta. Soil Biology and Biochemistry 46, 18–25. https://doi.org/10.1016/j.soilbio.2011.10.018.

Jackson, L.E., Calderon, F.J., Steenwerth, K.L., Scow, K.M., Rolston, D.E., 2003. Responses of soil microbial processes and community structure to tillage events and implications for soil quality. Geoderma 114 (3–4), 305–317. https://doi.org/10.1016/S0016-7061(03)00046-6.

Janz, B., Havermann, F., Lashermes, G., Zuazo, P., Engelsberger, F., Torabi, S.M., Butterbach-Bahl, K., 2022. Effects of crop residue incorporation and properties on combined soil gaseous N2O, NO, and NH3 emissions-A laboratory-based measurement approach. The Science of the Total Environment 807 (Pt 2), 151051. https://doi.org/10.1016/j.scitotenv.2021.151051.

Jones, C.M., Spor, A., Brennan, F.P., Breuil, M.C., Bru, D., Lemanceau, P., Griffiths, B., Hallin, S., Philippot, L., 2014. Recently identified microbial guild mediates soil N2O sink capacity. Nature Climate Change. https://doi.org/10.1038/nclimate2301.

Kalbitz, K., Schmerwitz, J., Schwesig, D., Matzner, E., 2003. Biodegradation of soil-derived dissolved organic matter as related to its properties. Geoderma. https://doi.org/10.1016/S0016-7061(02)00365-8.

Kandeler, E., Deiglmayr, K., Tscherko, D., Bru, D., Philippot, L., 2006. Abundance of narG, nirS, nirK, and nosZ genes of denitrifying bacteria during primary successions of a glacier foreland. Applied and Environmental Microbiology. https://doi.org/10.1128/AEM.00439-06.

Kramer, C., Gleixner, G., 2008. Soil organic matter in soil depth profiles: distinct carbon preferences of microbial groups during carbon transformation. Soil Biology and Biochemistry. https://doi.org/10.1016/j.soilbio.2007.09.016.

Lashermes, G., Recous, S., Alavoine, G., Janz, B., Butterbach-Bahl, K., Ernfors, M., Laville, P., 2022. N2O emissions from decomposing crop residues are strongly linked to their initial soluble fraction and early C mineralization. Science of the Total Environment 806, 150883. https://doi.org/10.1016/j.scitotenv.2021.150883.

Lee, Y.B., Lorenz, N., Dick, L.K., Dick, R.P., 2007. Cold storage and pretreatment incubation effects on soil microbial properties. Soil Science Society of America Journal 71 (4), 1299–1305. https://doi.org/10.2136/sssaj2006.0245.

Lemke, R.L., Liu, L., Baron, V.S., Malhi, S.S., Farrell, R.E., 2018. Effect of crop and residue type on nitrous oxide emissions from rotations in the semi-arid Canadian prairies. Canadian Journal of Soil Science. https://doi.org/10.1139/cjss-2018-0001.

Li, G.D., Schwenke, G.D., Hayes, R.C., Lowrie, A.J., Lowrie, R.J., Poile, G.J., Oates, A.A., Xu, B., Rohan, M., 2021. Can legume species, crop residue management or no-till mitigate nitrous oxide emissions from a legume-wheat crop rotation in a semi-arid environment? Soil and Tillage Research 209, 104910. https://doi.org/10.1016/j.still.2020.104910.

Li, X., Hu, F., Shi, W., 2013. Plant material addition affects soil nitrous oxide production differently between aerobic and oxygen-limited conditions. Applied Soil Ecology. https://doi.org/10.1016/j.apsoil.2012.10.003.

Li, Z., Reichel, R., Xu, Z., Vereecken, H., & Brüggemann, N. (n.d.). Return of crop residues to arable land stimulates N 2 O emission but mitigates NO 3 − leaching: A meta-analysis. https://doi.org/10.1007/s13593-021-00715-x/Published.

Linton, N.F., Ferrari Machado, P.V., Deen, B., Wagner-Riddle, C., Dunfield, K.E., 2020. Long-term diverse rotation alters nitrogen cycling bacterial groups and nitrous oxide emissions after nitrogen fertilization. Soil Biology and Biochemistry 149, 107917. https://doi.org/10.1016/j.soilbio.2020.107917.

Liu, L., Knight, J.D., Lemke, R.L., Farrell, R.E., 2024. Quantifying the contribution of above- and below-ground residues of chickpea, faba bean, lentil, field pea and wheat to the nitrogen nutrition of a subsequent wheat crop. Field Crops Research 313, 109412. https://doi.org/10.1016/j.fcr.2024.109412.

Ma, E., Zhang, G., Ma, J., Xu, H., Cai, Z., Yagi, K., 2010. Effects of rice straw returning methods on N2O emission during wheat-growing season. Nutrient Cycling in Agroecosystems. https://doi.org/10.1007/s10705-010-9369-1.

Macdonald, L.M., Paterson, E., Dawson, L.a., McDonald, A.J.S., 2004. Short-term effects of defoliation on the soil microbial community associated with two contrasting Lolium perenne cultivars. Soil Biology and Biochemistry 36 (3), 489–498. https://doi.org/10.1016/j.soilbio.2003.11.001.

Machado, P.V.F., Farrell, R.E., Deen, W., Voroney, R.P., Congreves, K.A., Wagner-Riddle, C., 2021. Contribution of crop residue, soil, and fertilizer nitrogen to nitrous oxide emissions varies with long-term crop rotation and tillage. Science of the Total Environment 767. https://doi.org/10.1016/j.scitotenv.2021.145107.

Masta, M., Espenberg, M., Kuusemets, L., Pärn, J., Thayamkottu, S., Sepp, H., Kirsimäe, K., Sgouridis, F., Kasak, K., Soosaar, K., Mander, Ü., 2023. 15N tracers and microbial analyses reveal *in situ* N2O sources in contrasting water regimes on drained peatland forest. Pedosphere. https://doi.org/10.1016/j.pedsph.2023.06.006.

McGill, W., Rutherford, P., Figueiredo, C., Arocena, J., 2007. Total nitrogen. In: Soil Sampling and Methods of Analysis, second ed. https://doi.org/10.1201/9781420005271.ch22

Miller, M.N., Zebarth, B.J., Dandie, C.E., Burton, D.L., Goyer, C., Trevors, J.T., 2008. Crop residue influence on denitrification, N2O emissions and denitrifier community abundance in soil. Soil Biology and Biochemistry. https://doi.org/10.1016/j.soilbio.2008.06.024.

Moore-Kucera, J., Dick, R.P., 2008. Application of 13C-labeled litter and root materials for *in situ* decomposition studies using phospholipid fatty acids. Soil Biology and Biochemistry. https://doi.org/10.1016/j.soilbio.2008.06.002.

Moreno-Cornejo, J., Zornoza, R., Doane, T.A., Faz, Á., Horwath, W.R., 2015. Influence of cropping system management and crop residue addition on soil carbon turnover through the microbial biomass. Biology and Fertility of Soils. https://doi.org/10.1007/s00374-015-1030-3.

Mutegi, J.K., Munkholm, L.J., Petersen, B.M., Hansen, E.M., Petersen, S.O., 2010. Nitrous oxide emissions and controls as influenced by tillage and crop residue management strategy. Soil Biology and Biochemistry 42 (10), 1701–1711. https://doi.org/10.1016/j.soilbio.2010.06.004.

Németh, D.D., Wagner-Riddle, C., Dunfield, K.E., 2014. Abundance and gene expression in nitrifier and denitrifier communities associated with a field scale spring thaw N2O

flux event. Soil Biology and Biochemistry. https://doi.org/10.1016/j.soilbio.2014.02.007.
Pascault, N., Ranjard, L., Kaisermann, A., Bachar, D., Christen, R., Terrat, S., Mathieu, O., Lévêque, J., Mougel, C., Henault, C., Lemanceau, P., Péan, M., Boiry, S., Fontaine, S., Maron, P.A., 2013. Stimulation of different functional groups of bacteria by various plant residues as a driver of soil priming effect. Ecosystems. https://doi.org/10.1007/s10021-013-9650-7.
Phillips, R., Grelet, G., McMillan, A., Song, B., Weir, B., Palmada, T., Tobias, C., 2016. Fungal denitrification: bipolaris sorokiniana exclusively denitrifies inorganic nitrogen in the presence and absence of oxygen. FEMS Microbiology Letters. https://doi.org/10.1093/femsle/fnw007.
Reimer, J.C., Arcand, M.M., Helgason, B.L., 2023. Soil denitrification response to increased urea concentration constrains nitrous oxide emissions in a simulated cattle urine patch. Plant and Soil. https://doi.org/10.1007/s11104-023-06048-w.
Rochette, P., 2008. No-till only increases N2O emissions in poorly-aerated soils. Soil and Tillage Research. https://doi.org/10.1016/j.still.2008.07.011.
Sander, B.O., Samson, M., Buresh, R.J., 2014. Methane and nitrous oxide emissions from flooded rice fields as affected by water and straw management between rice crops. Geoderma. https://doi.org/10.1016/j.geoderma.2014.07.020.
Schaufler, G., Kitzler, B., Schindlbacher, A., Skiba, U., Sutton, M.A., Zechmeister-Boltenstern, S., 2010. Greenhouse gas emissions from European soils under different land use: effects of soil moisture and temperature. European Journal of Soil Science. https://doi.org/10.1111/j.1365-2389.2010.01277.x.
Schimel, J.P., Schaeffer, S.M., 2012. Microbial control over carbon cycling in soil. Frontiers in Microbiology 3 (SEP). https://doi.org/10.3389/fmicb.2012.00348.
Schwenke, G., Haigh, B., Mcmullen, G., Herridge, D., 2010. Soil nitrous oxide emissions under dryland N-fertilised canola and N 2 -fixing chickpea in the northern grains region, Australia. In: Proc. 19th World Congress of Soil Science, Soil Solutions for a Changing World.
Shan, J., Yan, X., 2013. Effects of crop residue returning on nitrous oxide emissions in agricultural soils. Atmospheric Environment 71, 170–175. https://doi.org/10.1016/j.atmosenv.2013.02.009.
Shang, Q., Yang, X., Gao, C., Wu, P., Liu, J., Xu, Y., Shen, Q., Zou, J., Guo, S., 2011. Net annual global warming potential and greenhouse gas intensity in Chinese double rice-cropping systems: a 3-year field measurement in long-term fertilizer experiments. Global Change Biology. https://doi.org/10.1111/j.1365-2486.2010.02374.x.
Shorunke, A., 2020. Influence of nitrogen application and crop residue on drivers of microbial nitrous oxide emissions in canola (Brassica napus L.) production.
Skjemstad, J.O., Baldock, J., 2007. Total and organic carbon. Soil Sampling and Methods of Analysis 225–237. https://doi.org/10.1201/9781420005271.ch21.
Surey, R., Schimpf, C.M., Sauheitl, L., Mueller, C.W., Rummel, P.S., Dittert, K., Kaiser, K., Böttcher, J., Mikutta, R., 2020. Potential denitrification stimulated by water-soluble organic carbon from plant residues during initial decomposition. Soil Biology and Biochemistry 147, 107841. https://doi.org/10.1016/j.soilbio.2020.107841.
Tatti, E., Goyer, C., Chantigny, M., Wertz, S., Zebarth, B.J., Burton, D.L., Filion, M., 2014. Influences of over winter conditions on denitrification and nitrous oxide-producing microorganism abundance and structure in an agricultural soil amended with different nitrogen sources. Agriculture, Ecosystems & Environment. https://doi.org/10.1016/j.agee.2013.10.021.
Tosi, M., Brown, S., Ferrari Machado, P.V., Wagner-Riddle, C., Dunfield, K., 2020. Short-term response of soil N-cycling genes and transcripts to fertilization with nitrification and urease inhibitors, and relationship with field-scale N2O emissions. Soil Biology and Biochemistry. https://doi.org/10.1016/j.soilbio.2019.107703.
Walter, K., Don, A., Fuß, R., Kern, J., Drewer, J., Flessa, H., 2015. Direct nitrous oxide emissions from oilseed rape cropping – a meta-analysis. GCB Bioenergy 7 (6), 1260–1271. https://doi.org/10.1111/gcbb.12223.
White, D.C., Davis, W.M., Nickels, J.S., King, J.D., Bobbie, R.J., 1979. Determination of the sedimentary microbial biomass by extractible lipid phosphate. Oecologia 40, 51–62.
Wu, X., Liu, H., Fu, B., Wang, Q., Xu, M., Wang, H., Yang, F., Liu, G., 2017. Effects of land-use change and fertilization on N2O and NO fluxes, the abundance of nitrifying and denitrifying microbial communities in a hilly red soil region of southern China. Applied Soil Ecology. https://doi.org/10.1016/j.apsoil.2017.08.004.
Xia, L., Wang, S., Yan, X., 2014. Effects of long-term straw incorporation on the net global warming potential and the net economic benefit in a rice-wheat cropping system in China. Agriculture, Ecosystems & Environment. https://doi.org/10.1016/j.agee.2014.08.001.
Yamamoto, A., Akiyama, H., Nakajima, Y., Hoshino, Y.T., 2017. Estimate of bacterial and fungal N 2 O production processes after crop residue input and fertilizer application to an agricultural field by 15 N isotopomer analysis. Soil Biology and Biochemistry. https://doi.org/10.1016/j.soilbio.2017.01.015.
Zhou, Z., Takaya, N., Sakairi, M.A.C., Shoun, H., 2001. Oxygen requirement for denitrification by the fungus Fusarium oxysporum. Archives of Microbiology. https://doi.org/10.1007/s002030000231.
Zsolnay, A., 1996. Dissolved humus in soil waters. Humic Substances in Terrestrial Ecosystems. https://doi.org/10.1016/b978-044481516-3/50005-0.
Zsolnay, Á., 2003. Dissolved organic matter: artefacts, definitions, and functions. Geoderma. https://doi.org/10.1016/S0016-7061(02)00361-0.
Zumft, W.G., 1997. Cell biology and molecular basis of denitrification. Microbiology and Molecular Biology Reviews: Microbiology and Molecular Biology Reviews.